



1 **Relevance of feedbacks between water availability and crop**
2 **systems using a coupled hydrology – crop growth model**

3 Sneha Chevuru¹, L.P.H. (Rens) van Beek¹, Michelle T.H. van Vliet¹, Jerom P.M. Aerts^{2&3},
4 Marc F.P. Bierkens^{1&4}

5 ¹ Department of Physical Geography, Utrecht University, The Netherlands.

6 ² Water Resources Section, Faculty of Civil Engineering and Geosciences, Delft University of Technology, The
7 Netherlands

8 ³ Department of Hydraulic Engineering, Faculty of Civil Engineering and Geosciences, Delft University of
9 Technology, The Netherlands

10 ⁴ Unit Subsurface & Groundwater Systems, Deltares, Utrecht, The Netherlands

11

12 *Correspondence to:* Sneha Chevuru (s.chevuru@uu.nl)

13

14 **Abstract**

15 Individual hydrological and crop growth models often oversimplify underlying processes,
16 reducing the accuracy of both simulated hydrology and crop growth dynamics. While crop
17 models tend to generalize soil moisture processes, most hydrological models commonly use
18 constant vegetation parameters and prescribed phenologies, neglecting the dynamic nature of
19 crop growth. Despite some studies that have coupled hydrological and crop models, a limited
20 understanding exists regarding the feedbacks between hydrology and crop growth. Our
21 objective is to quantify the feedback between crop systems and hydrology on a fine-grained
22 spatio-temporal level. To this end, the PCR-GLOBWB 2 hydrological model was coupled with
23 the WOFOST crop growth model to quantify both the one-way and two-way interactions
24 between hydrology and crop growth on a daily timestep and at 5 arc minutes (~10 km)
25 resolution. Our study spans the Contiguous United States (CONUS) region and covers the
26 period from 1979 to 2019, allowing a comprehensive evaluation of the feedback between
27 hydrology and crop growth dynamics. We compare individual (stand-alone) as well as one-
28 way and two-way coupled WOFOST and PCR-GLOBWB 2 model runs and evaluate the
29 average crop yield and its interannual variability for rainfed and irrigated crops as well as
30 simulated irrigation water withdrawal for maize, wheat and soybean. Our results reveal distinct
31 patterns in the temporal and spatial variation of crop yield depending on the included
32 interactions between hydrology and crop systems. Evaluating the model results against
33 reported yield and water use data demonstrates the efficacy of the coupled framework in
34 replicating observed irrigated and rainfed crop yields. Our results show that two-way coupling,
35 with its dynamic feedback mechanisms, outperforms one-way coupling for rainfed crops. This
36 improved performance stems from the feedback of WOFOST crop phenology to the crop
37 parameters in the hydrological model. Our results suggest that when crop models are combined



38 with hydrological models, a two-way coupling is needed to capture the impact of interannual
39 climate variability on food production.

40

41

42 **1 Introduction**

43 Global trends in population and economic growth are expected to increase the demand for
44 water, food, and energy, threatening the sustainable and equitable use of natural resources
45 (Sophocleous, 2004; Tompkins and Adger, 2004). Water as a resource plays a crucial role in
46 crop growth, cooling of thermoelectric plants, hydropower generation, and covering domestic
47 and industrial demand. Water, therefore, is an essential resource at the core of the Water-
48 Energy-Food-Ecosystem (WEFE) nexus. Currently, 70% of total global freshwater
49 withdrawals are accounted for by agriculture, making it the largest water user among all sectors
50 (Dubois, 2011). The Food and Agriculture Organization (FAO) of the United Nations estimated
51 that the demand for water and food resources will likely increase by 50% by 2050 compared
52 to 2015 (IRENA, 2015; Corona-López et al., 2021). The increasing demand for water and food
53 will likely have negative impacts on the environment and will inhibit socio-economic
54 development if a gap opens between growing water demand and water availability.

55 The critical interplay between hydrology and crop growth becomes evident during
56 hydroclimatic extremes (e.g. droughts, heatwaves), as rising demands coincide with potential
57 declines in both water resources and food production (crop yield) (Jackson et al., 2021). In
58 addressing the complexities associated with these challenges, studies by Jägermeyr et al.
59 (2017), utilizing a dynamic vegetation model (LPJmL), evaluated achievable irrigated crop
60 production under sustainable water management. Their findings revealed that 41% of global
61 water use currently compromises environmental flow requirements crucial for river
62 ecosystems, potentially leading to losses in irrigated croplands. Concurrently, research by
63 Vörösmarty et al. (2000) and Leclère et al., (2014) projects the impacts of climate change on
64 global agricultural systems, foreseeing an increase in irrigated areas in the future, underscoring
65 the necessity for significant investments in irrigation, energy, and water resource management.

66 Biophysical process-based models, as highlighted by Siad et al., (2019) and Zhang et al.,
67 (2021), are instrumental in understanding the intricate relationship between hydrology and crop
68 growth, particularly in response to changing hydroclimatic conditions. Considering factors like
69 irrigation water use and soil-groundwater dynamics, these models explore how meteorological



70 events influence water availability for crops, as well as the impacts of diminished growth and
71 premature senescence on hydrology through effects on root water uptake and
72 evapotranspiration. This understanding becomes crucial when assessed at the regional to global
73 scale, where local deficits can have cascading consequences for both water and food security.

74 In the context of studying the impact of climate change and variability on crop yields, aside
75 from biophysical models, numerous crop models have been employed. However, these models
76 often incorporate a simplified soil-water balance (Zhang et al., 2021) that overlooks local
77 hydrological processes and often do not account for water use for irrigation and non-
78 agricultural sectors. Conversely, most hydrological models simplify or neglect the effects of
79 land cover, phenology and vegetation changes on hydrological fluxes and the state of available
80 water resources (Tsarouchi et al., 2014). These simplifications arise due to computational
81 expediency, disparities in process scales between hydrology at the river basin level and crop
82 yield at the field level, incomplete understanding of the other domain by model developers, or
83 because of epistemological uncertainty (Siad et al. 2019; McMillan et al., 2018; Shafiei et al.
84 2014). Recognizing the strengths of both crop models and global hydrological models, a
85 coupling allows for the exploration of dynamic crop growth's influence on hydrology and water
86 use and the incorporation of accurate spatio-temporal variations in hydrological fluxes,
87 including water use, in estimates of crop yield.

88 Noteworthy efforts by Droppers et al. (2021) have successfully coupled hydrological and crop
89 models, primarily focusing on achieving attainable crop production. However, these efforts
90 were conducted at half-degree (~50 km) spatial resolution and focused on long-term average
91 crop yield. They therefore fall short in exploring the aspects of fine-scale spatiotemporal
92 variability in particular as a result of interannual climate variability. Other recent efforts to
93 couple crop growth models and global hydrological models (Jägermeyr et al., 2017)
94 predominantly focus on assessing yield under different scenarios or adaptation measures.
95 However, limited work focused on delving into how two-way interactions and feedback
96 mechanisms between crop growth and hydrological systems operate.

97 In addition, integrated assessment models have been instrumental in studying the combined
98 effects of climate change and socio-economic developments on crop yield and water resources
99 at a large scale. Typically, these models operate on a macro-regional level (Easterling, 1997)
100 and use annual (or 5 to 10 yearly timesteps), neglecting the impacts of inter- and intra-annual
101 variability and particularly short-term hydroclimatic extremes. Furthermore, integrated



102 assessment models often adopt an optimization modelling approach, making them less suitable
103 for studying the effects of hydroclimatic extremes (Ewert et al., 2015).

104 Another class of efforts to link water to crop production are water-food nexus studies, that,
105 however, tend to concentrate on local linkages or provide qualitative descriptions of existing
106 connections (Momblanch et al., 2019). For instance, a recent review of water-food nexus
107 studies focusing on the contiguous United States (CONUS), shows that such studies focus
108 mainly on water security indicators (Veetil et al., 2022) or climate variability impacts on crop
109 yields (Huang et al., 2021). However, knowledge gaps persist, as water and food resources are
110 often evaluated separately (Corona-López et al., 2021), exploring allocations through an
111 optimization model (Mortada et al., 2018) that lacks spatiotemporal variability considerations.
112 Notably, there is a lack of effort to understand the interactions between hydrology and crop
113 growth. Further research is needed to bridge these gaps and enhance our understanding of the
114 dynamic and interlinked processes shaping the water-food nexus.

115 To address this knowledge gap, our objective is, therefore, to quantify the feedback between
116 crop growth and hydrology. Although eventually global scale in scope, we limit this analysis
117 to the Contiguous United States (CONUS) region, to keep the analysis tractable and because
118 CONUS has detailed information on yearly crop production and water use.

119 CONUS is a major producer and contributor to the global production of three primary crops:
120 maize, soybean, and wheat. These crops were selected due to their substantial impact on the
121 agricultural landscape and their pivotal role in shaping global food production trends. The
122 CONUS serves as an ideal study area owing to its extensive availability of relevant data,
123 particularly on agricultural statistics and irrigation water withdrawals, which can provide a
124 basis for analysis and model evaluation. Additionally, the CONUS region exhibits diverse
125 climatic and geographic conditions, contributing to a better understanding of crop and water
126 system dynamics and their responses to various environmental factors.

127 To this end, we developed a coupled global hydrological-crop growth model framework to
128 answer questions related to 1) the impacts of irrigation and hydrology on crop growth; 2) the
129 feedbacks of crop growth on the hydrological system when accounting for interannual
130 variability; and 3) the importance of the two-way coupling between hydrology and crop growth
131 to provide realistic water resources and crop yield simulations. By delving into these aspects,
132 we aim to contribute valuable insights into the feedback processes between hydrology and crop
133 growth, thereby addressing the current research gap in a more comprehensive manner.



134 To address this, the PCR-GLOBWB 2 hydrological model (Sutanudjaja et al., 2018) is coupled
135 to the WOFOST crop model (de Wit et al., 2019) at a daily timestep and at 5 arc minutes (~10
136 km) spatial resolution applied to CONUS (section 2.1). First, a one-way coupling is established
137 to evaluate the effect of the simulated water availability of PCR-GLOBWB 2 for rainfed and
138 irrigated crop growth in WOFOST (section 2.1; section 2.2.1). In addition, a two-way coupling
139 is established in which, additional to passing water availability from PCR-GLOBWB 2 to
140 WOFOST, the crop phenology of WOFOST in terms of actual evapotranspiration, leaf area
141 index and rooting depth is fed back into PCR-GLOBWB 2 (section 2.1, 2.2.2;). Furthermore,
142 individual WOFOST and coupled one-way and two-way model runs were compared to
143 evaluate the impacts of feedbacks on crop yield and irrigation water use (section 2.3). The
144 results of these simulations are compared with and evaluated against reported yield statistics
145 and reported annual irrigation withdrawals to assess their validity (section 2.4; section 3). In
146 the end, we elaborate on the uncertainties, strengths, and usability of our coupled model
147 framework for studying the water-food nexus under global change (section 4).

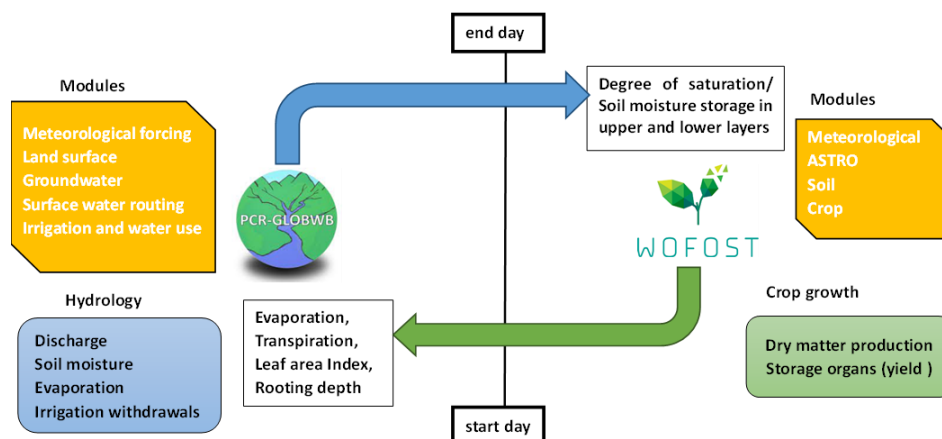
148

149 **2 Methods**

150 **2.1 Coupled PCR-GLOBWB 2-WOFOST model framework**

151 A new fully coupled PCR-GLOBWB 2 - WOFOST model framework is developed to include
152 the feedbacks between crop growth and hydrology. Here, we included both a one-way and two-
153 way coupling between the PCR-GLOBWB 2 global hydrology and water resources model
154 (Sutanudjaja et al., 2018) and the WOFOST crop growth model (de Wit et al., 2019). This
155 coupled framework was then used to quantify the impacts of included feedbacks between
156 hydrology and crop growth on a daily timestep and 5 arcminutes resolution for CONUS. The
157 following (sub)sections provide a description of the PCR-GLOBWB 2 and WOFOST models
158 and modules used (2.1), the model coupling setup (2.2), model coupling simulation
159 experiments and parametrization (2.3), validation of crop yield and of irrigation water use (2.4).

160



161

162 **Figure 1:** The coupled model framework of the PCR-GLOBWB 2 hydrology and water resources model
163 and the WOFOST crop growth model. The blue arrow represents the one-way coupling from PCR-
164 GLOBWB 2 to WOFOST and the variables that are exchanged; the green arrow is added in case the full
165 two-way coupling is considered. At the start of the day, WOFOST computes evapotranspiration, leaf area
166 index, and rooting depth that is used by PCR-GLOBWB 2 to compute soil moisture status. At the end of
167 the day, soil moisture storage in the upper and lower layers from PCR-GLOBWB 2 is fed to WOFOST to
168 compute crop growth for the next day.

169 PCR-GLOBWB 2

170 The PCRaster Global Water Balance (PCR-GLOBWB 2) model (Sutanudjaja et al., 2018) is a
171 global hydrology and water resource model developed at Utrecht University. This model
172 operates on a latitude-longitude grid for which it simulates fluxes and stores of the terrestrial
173 hydrological cycle with a daily resolution and dynamically includes anthropogenic impacts
174 such as man-made reservoirs and sectoral water demands, water withdrawals, consumptive
175 water use, and return flows. The PCR-GLOBWB 2 model currently consists of five main
176 hydrological modules encompassing meteorological forcing, land surface, groundwater,
177 surface water, irrigation and water use (Fig. 1).

178 The PCR-GLOBWB 2 meteorological forcing uses a gridded time series of temperature and
179 precipitation as input. More information on input datasets is provided in supplementary I.
180 Reference potential evaporation is computed within the model using Hamon's (1963) method.
181 The resulting reference potential evaporation is then employed in the land surface module to
182 calculate the crop-specific land cover potential evaporation. Separate soil conditions are
183 specified for each land cover type, with vegetative and soil properties varying accordingly for
184 each grid cell and land cover type. The groundwater and surface water modules simulate the
185 fluxes and stores of groundwater and surface water, respectively. The irrigation and water use
186 module focuses on simulating water demand, withdrawals, consumption, and return flows. For



187 a more detailed understanding of each module, we refer to the comprehensive description
188 provided by Sutanudjaja et al. (2018).

189 **WOFOST**

190 WOFOST (WORld FOod STudies) is a crop simulation model developed at Wageningen
191 ‘School of De Wit’, in the Netherlands, designed to quantitatively analyze the crop growth and
192 potential production of annual field crops at the field scale (Supit et al., 1994). WOFOST
193 employs a fixed time step of one day to simulate crop growth based on eco-physiological
194 processes such as phenological development and growth (de Wit et al., 2019). WOFOST has
195 found extensive application in assessing the impacts of climate change and management
196 strategies on crop growth and yield at local to global scales.

197 The WOFOST crop model comprises of four modules: weather, crop, astro and soil (Fig. 1).
198 The WOFOST modules simulate a range of processes, including phenological development,
199 CO₂ assimilation, leaf development, light interception, transpiration, respiration, root growth,
200 assimilated partitioning to the various organs and the formation of dry matter. The model’s
201 output includes simulated crop biomass total, crop yield and variables such as leaf area and
202 crop water use.

203 **2.2 Model coupling setup**

204 The PCR-GLOBWB 2 - WOFOST coupled model framework integrates hydrological and crop
205 models through both one-way and two-way couplings, as illustrated in Fig. 1. This model
206 coupling aims to assess the intricate interactions between hydrology and crop growth under
207 different agricultural conditions, specifically irrigated and rainfed settings. The one-way
208 coupling examines the impact of water availability on crop growth, while the two-way coupling
209 incorporates the exchange of soil moisture status and hydrological parameters and fluxes based
210 on crop status.

211 The online coupling process occurs seamlessly at each time step, facilitating dynamic
212 interactions between WOFOST and PCR-GLOBWB 2 and limiting I/O-related computation
213 times. To achieve this integration, we utilized the Basic Model Interface (BMI) (Hutton et al.,
214 2020; Peckham et al., 2013), which is particularly valuable as WOFOST and PCR-GLOBWB
215 2 are written in different programming languages (C and PCRaster-Python, respectively). The
216 decision to use BMI was driven by its non-interfering nature, ensuring no code entanglement
217 and facilitating seamless connection between the models. BMI functions act as a bridge,



218 enabling direct variable exchange between WOFOST and PCR-GLOBWB 2 without
219 modifying their source code. This non-invasive approach ensures a flexible and robust coupling
220 framework, allowing for continuous model development without interruptions. Integrating
221 BMI functions into both models provides a set of functions for retrieving or altering model
222 variables, enhancing adaptability and efficiency. The schematization of the workflow of the
223 coupled PCR-GLOBWB 2 - WOFOST model framework can be seen in Supplementary
224 Information II Fig. S1. Further details on BMI functions used for the development of the
225 coupled PCR-GLOBWB 2 – WOFOST model framework are available in supplementary II.

226 **2.2.1 One-way coupling**

227 In the one-way coupling, information on soil hydrology is passed from PCR-GLOBWB 2 to
228 WOFOST (Fig 1). Here, PCR-GLOBWB 2 simulates soil moisture content for every day and
229 the soil water storage is simulated separately for each land cover type. Consequently, WOFOST
230 receives the soil moisture content from PCR-GLOBWB 2 as input, with generally higher values
231 of soil moisture for irrigated crops than of nearby rainfed crops. WOFOST then simulates the
232 crop yield based on the simulated soil moisture content and the same meteorological inputs as
233 PCR-GLOBWB 2 uses.

234 The combined model framework captures the impact of hydroclimatic conditions by assessing
235 water stress and heat stress. Water stress, influenced by soil moisture levels derived from PCR-
236 GLOBWB 2, affects various processes in WOFOST such as a reduction in the leaf area, a
237 decrease in the assimilation of biomass (growth), changes in the partitioning of biomass, and
238 an increase in various plant organs of senescence (ageing processes). Elevated temperatures
239 have varying effects across different stages of crop development. They can accelerate crop
240 growth by promoting faster accumulation of Growing Degree Days, which are essential for
241 determining crop maturity. However, prolonged exposure to high temperatures can also induce
242 heat stress, adversely impacting crop health and potentially shortening the overall duration of
243 the crop's growth cycle. Insufficient water availability that limits the evapotranspiration also
244 reduces the amount of assimilation and the corresponding yield.

245 **2.2.2 Two-way coupling**

246 In addition to one-way coupling, vegetation-related states and fluxes are passed from WOFOST
247 to PCR-GLOBWB 2 and data exchange between the two models is iterated twice per day. In
248 the two-way coupling, information is exchanged between PCR-GLOBWB 2 and WOFOST as
249 follows (Fig. 1):



- 250 • At the start of the day, WOFOST computes the potential evapotranspiration on the basis
251 of the meteorological variables and the pertinent vegetation states from the previous
252 time step (leaf area index (LAI), rooting depth, and crop height), as well as the actual
253 bare soil evaporation, actual transpiration and the open water evaporation;
- 254 • The fluxes are passed to PCR-GLOBWB 2, together with the root depth. The root depth
255 is used to partition the actual transpiration from the single root zone of WOFOST over
256 the two soil layers of PCR-GLOBWB 2, dependent on the root content. For both
257 irrigated and rainfed crops, the actual evapotranspiration from WOFOST is imposed on
258 PCR-GLOBWB 2 and used to update the soil moisture content of the two soil layers in
259 PCR-GLOBWB 2 for the current daily timestep;
- 260 • In the case of irrigated crops, the stages of vegetated development are used to compute
261 the amount of irrigation. Potential evaporation is used to calculate the irrigation water
262 demand for paddy crops (not considered here), whereas the irrigation water requirement
263 for non-paddy crops is computed on the basis of the soil moisture status according to
264 the FAO guidelines (Allen et al., 1998). The irrigation water requirement is withdrawn
265 from the available water resources in PCR-GLOBWB 2 and the available irrigation
266 water supply is applied to the crops in addition to any natural precipitation;
- 267 • The resulting soil moisture of the two soil layers from PCR-GLOBWB 2 is aggregated
268 to the average value for the root zone of each crop and passed to WOFOST;
- 269 • With the soil moisture from PCR-GLOBWB 2, WOFOST computes the actual
270 transpiration and the crop growth and the crop status is updated. The new fluxes and
271 new crop parameters are then passed to PCR-GLOBWB 2 again in the next daily
272 timestep (Fig.1).

273 In this two-way coupling, the crop phenology from WOFOST determines evapotranspiration
274 and thus the soil hydrology of PCR-GLOBWB 2, particularly during dry spells. Compared to
275 the predefined phenology of PCR-GLOBWB 2, the LAI, rooting depth and evapotranspiration
276 as simulated by WOFOST will lag during dry spells and less water may be lost from PCR-
277 GLOBWB 2. However, the thinner rooting depth will also lead to an earlier drying out of the
278 soil and reduced capillary rise. This subsequently leads to reduced soil moisture (compared to
279 PCR-GLOBWB 2 standalone) which in turn feeds back to a reduced simulated yield in
280 WOFOST, in particular for rainfed crops. For irrigated crops, the extra water supplied will
281 largely offset these feedbacks and result in near-optimum growth.

282 **2.3 Model coupling simulation experiments and parametrization**



283 Hydrological simulations were conducted with a daily timestep at a 5-arcminute grid
284 resolution, where for each grid cell WOFOST was used to simulate crop growth for irrigated
285 and rainfed maize, soybean, and wheat. To assess the impact of hydrology on crop growth and
286 understand the interactions between hydrology and crop growth, three sets of simulations were
287 carried out for both irrigated and rainfed crops: a) standalone simulations using the WOFOST
288 crop model solely, b) one-way coupled, and c) two-way coupled PCR-GLOBWB 2 - WOFOST
289 simulations. Note that for the standalone simulations with WOFOST under irrigation the
290 potential crop yield is simulated, which is potential yield without water (and nutrient) stress
291 except for temperature effects. When coupled to PCR-GLOBWB 2, water stress can occur even
292 for irrigated crops in case there is not enough water available (in PCR-GLOBWB 2) to fully
293 satisfy the crop water demand. For rainfed crops, growth is influenced by available soil
294 moisture for all simulations and is thus sensitive to water stress and temperature. Green water
295 from natural rainfall is the primary water supply in rainfed analysis, while irrigated crops get
296 water from both green and blue water (from surface water and renewable groundwater) and
297 non-renewable groundwater leading to groundwater depletion.

298 Daily timestep simulations covered the period from 1979 and 2019, using weather variables
299 (minimum and maximum air temperature, short wave radiation, precipitation, vapour pressure,
300 windspeed, and humidity) from the W5E5 forcing data (Lange et al., 2021) as input to PCR-
301 GLOBWB 2 (Sutanudjaja et al., 2018) and WOFOST. Cropland areas and growing seasons
302 were determined from the MIRCA2000 (Portmann et al., 2010) global monthly irrigated and
303 rainfed crop area dataset. The focus of the coupled framework was to comprehend the impacts
304 and feedback between hydrology and crop growth. Crop parameters, atmospheric CO₂
305 concentrations, and fertilizer application were obtained from the WOFOST crop parameter
306 dataset for each crop (WOFOST Crop Parameters, 2024). Cultivars in the WOFOST crop
307 parameter datasets were calibrated for each crop against reported agricultural yields from the
308 United States Department of Agriculture (USDA) National Agricultural Statistics Service
309 (USDA, 2024), with the closest matching cultivar selected for final simulations. Detailed
310 information on the cultivar calibration for each crop (i.e. irrigated and rainfed maize, soybean
311 and wheat) is provided in the supplementary information section III.

312 Comparisons were made between simulations from standalone WOFOST and the one-way and
313 two-way coupled PCR-GLOBWB 2 - WOFOST runs. This comparative analysis involved
314 evaluating the results from different model runs for crop growth against reported crop yields.



315 Furthermore, irrigation water withdrawals of coupled model runs are compared against the
316 USGS Water Use Database (USGS, 2023) (section 2.4).

317 **2.4 Model evaluation**

318 We evaluated the three different model configurations by comparing simulated results against
319 reported USDA crop yields of maize, soybean and wheat. Furthermore, we cross-referenced
320 our simulations with irrigation water withdrawal data spanning five years from the USGS
321 Water Use Database. Specifically, we compared data for the years 2005, 2010, and 2015, as
322 the USGS census data is collected at five-yearly intervals.

323 **2.4.1 Crop yields model evaluation**

324 To assess the model's performance, we employ three key metrics: correlation coefficients (r),
325 Normalized Root Mean Square Error (NRMSE) and Normalized Bias (NBIAS). These metrics
326 were selected for their ability to capture the strength, accuracy and systematic errors in the
327 relationship between simulated and observed values.

$$328 \quad r = \frac{\sum(P_i - \bar{P})(O_i - \bar{O})}{\sqrt{\sum(P_i - \bar{P})^2 \cdot \sum(O_i - \bar{O})^2}} \quad (1)$$

$$329 \quad NRMSE = \frac{\sqrt{\frac{1}{n} \sum_{i=1}^n (P_i - O_i)^2}}{\bar{O}} \quad (2)$$

$$330 \quad NBIAS = \frac{\frac{1}{n} \sum_{i=1}^n (P_i - O_i)}{\bar{O}} \quad (3)$$

331 Where, P_i and O_i are the individual predicted and observed values, respectively and \bar{P} and \bar{O}
332 are the means of the predicted and observed values.

333 The evaluation was done both temporally for average CONUS yields per year, as well as for
334 multi-year averages per state-per-state to evaluate the model's ability to capture spatial
335 variations in crop yield. This was done for both irrigated and rainfed maize, soybean and wheat.

336 To further characterize the dataset and evaluate the impact of the degree of coupling on
337 simulated yields, additional statistical analyses were conducted on the 41 years of simulated
338 data at the 5-arcminute grid scale. To this end, the mean and coefficient of variation (CV) were
339 computed for both one-way and two-way datasets for the three crops under irrigated and rainfed
340 conditions. The purpose of this analysis was to examine the central tendency and year-to-year
341 variability of yield simulations and how these are related to the way hydrology and crop growth
342 are coupled.



343 **2.4.2 Irrigation water use model evaluation**

344 The USGS reported irrigation water use data provides a comprehensive representation of the
345 total irrigation water utilized by all crops for a number of states (USGS, 2023). The irrigated
346 crop area used in this dataset is however not the same as that used in PCR-GLOBWB 2 which
347 is based on MIRCA2000 (Portmann et al., 2010). Thus, directly comparing USGS data with
348 our simulated water withdrawals would result in bias. To ensure a fair comparison between the
349 simulated and reported data, we adjusted the USGS irrigation water use data by multiplying
350 these with the ratio of the irrigated area from MIRCA2000 to the reported total USGS irrigated
351 area. Additionally, our simulated irrigation water withdrawal volumes did not yet account for
352 irrigation efficiency. We intend to implement this in future development. Hence, we introduced
353 an additional correction by dividing the simulated withdrawal data by the irrigation efficiency
354 as is commonly used in PCR-GLOBWB 2 when it is not coupled to a crop model.

355 After these corrections, the coupled model simulated irrigation water withdrawals were
356 evaluated against actual irrigation data obtained from the USGS database through spatial
357 (multi-year averages per state) and temporal (multi-state totals per year) analysis, providing
358 insights into the model's ability to replicate observed irrigation water use patterns.

359 This comparison was limited to the years with available reported area data for the simulation
360 period (2005, 2010, 2015) and to the states with reported irrigation water withdrawal volumes
361 for these years (37 states).

362 **3. Results**

363 In this section, we present the key findings obtained from the implementation of the coupled
364 hydrological-crop growth model framework based on WOFOST and PCR-GLOBWB 2. We
365 present our findings sequentially, first delving into observed hydrological impacts on crop
366 growth (one-way coupling) and then exploring how feedback mechanisms between crop
367 growth and hydrology impact the crop growth system (two-way coupling).

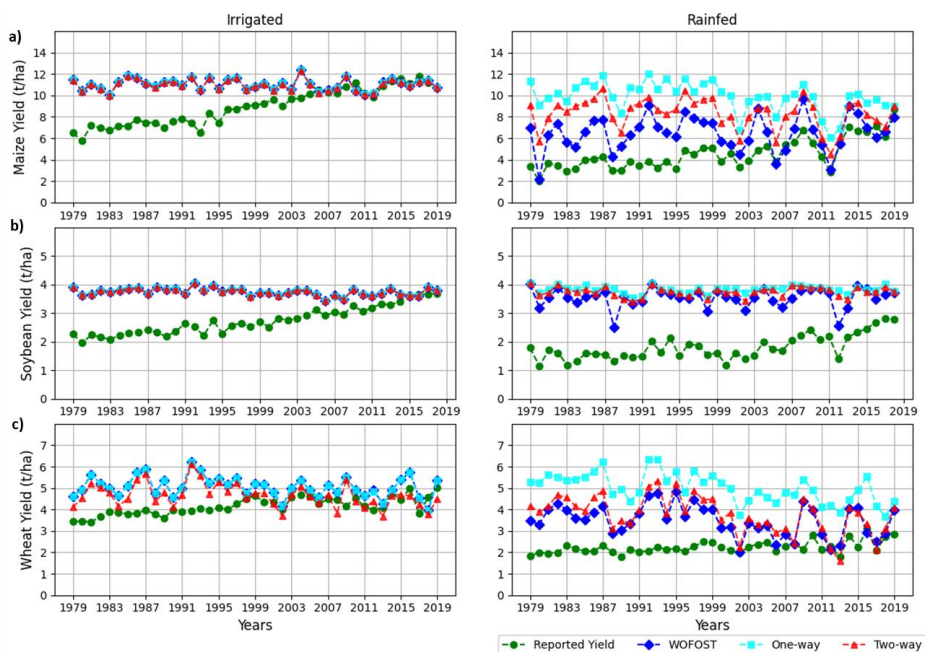
368 **3.1 Comparative temporal and spatial analysis of stand-alone, one-way, and two-way
369 coupling for irrigated and rainfed crops**

370 Temporal analysis (Fig. 2) compares the simulated yields with reported yields for irrigated and
371 rainfed maize, soybean, and wheat crops spanning from 1979 to 2019 in the CONUS region.
372 Notably, the reported yields exhibit discernible trends for the CONUS region across the three
373 crops and in both irrigated and rainfed analysis. This temporal evolution is primarily attributed



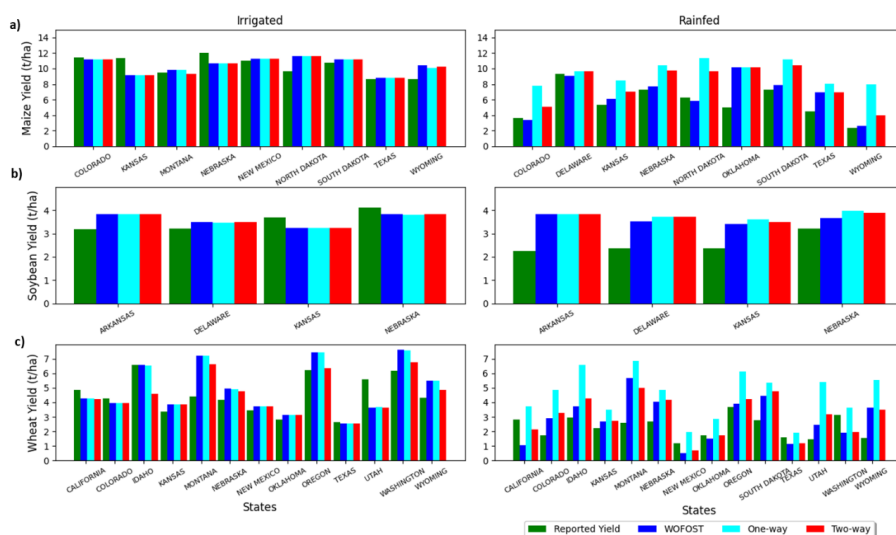
374 to technological advancements, encompassing improved agricultural practices and the
375 introduction of enhanced crop varieties over the study period (Arata et al., 2020).

376 In contrast, our coupled PCR-GLOBWB 2 – WOFOST model framework simulated yields do
377 not capture such trends, as the modelling approach intentionally omitted to incorporate trends
378 in technology and management practices. For a consistent analysis, we specifically focused on
379 the years when reported yields appear to be more or less stable and in line with our simulated
380 yields. Consequently, the timeframe from 2006 to 2019 was selected for further analysis. Thus,
381 to ensure a meaningful comparison, only the reported yields from 2006-2019 were used for
382 evaluating the accuracy and reliability to ensure a fair and meaningful comparison of simulated
383 yields.



384

385 **Figure 2: Temporal analysis of irrigated and rainfed crops of a) maize, b) soybean and c) wheat for the**
386 **years 1979 to 2019 of a CONUS region**



387

388 **Figure 3: Spatial (i.e. state level) analysis of irrigated and rainfed crops of a) maize, b) soybean and c) wheat**
 389 **for the years 2006 to 2019 for the CONUS region.**

390 Figures 2 and 3 show the outcomes of comparing simulated irrigated and rainfed analyses
 391 yields for maize, soybean, and wheat with reported yields. For the irrigated crops, the obtained
 392 yields by standalone WOFOST represent the potential productivity for the three crops. Notably,
 393 one-way, and two-way model runs for irrigated crops yielded nearly identical results to the
 394 standalone runs, indicating that there is generally enough irrigation water to completely satisfy
 395 crop water demands. Although not shown here, we note that this is at the expense of non-
 396 renewable groundwater use in states overlying the Southern Great Plains aquifer system.
 397 Conversely, for rainfed crops, the stand-alone and two-way simulations produced comparable
 398 results, while the one-way coupling approach exhibited an overestimation of yields relative to
 399 stand-alone and two-way simulations particularly for wheat and to a lesser degree for maize.
 400 This discrepancy arises from the fact that in one-way coupling soil moisture calculations in
 401 PCR-GLOBWB 2 under drought conditions assume a full rooting depth development (the
 402 phenology is fixed) which could, as described before, lead to an over-estimation of soil
 403 moisture that is then passed to WOFOST, eventually leading to an overestimation of yield. In
 404 contrast, the two-way coupling approach feeds back information about the lagging behind of
 405 crop development to PCR-GLOBWB 2, which results in more realistic soil moisture and crop
 406 yield simulations by the two-way coupling.

407 The analysis of temporal variations in simulated irrigated and rainfed maize crop yields shows
 408 distinct year-to-year fluctuations. Rainfed maize, in particular, exhibits a discernible pattern



409 with certain years marked by notable peaks in yields, contrasting with others that experienced
410 comparatively lower production, revealing sensitivity to varying environmental conditions.
411 These variations are also observed in reported maize yields. Similar year-to-year patterns are
412 found for simulated irrigated and rainfed wheat yields, but not so in observed yields.
413 Apparently, sensitivity to water and/or temperature variability in WOFOST is larger than
414 observed. Also, a significant discrepancy emerges in irrigated and rainfed soybean yields,
415 where simulated yields surpass the reported values, particularly in rainfed conditions.

416 In the spatial analysis, simulated irrigated maize yields from stand-alone (WOFOST), one-way,
417 and two-way coupling align almost identical with reported irrigated maize yields. Conversely,
418 in rainfed maize analysis, stand-alone and two-way simulations outperform reported yields in
419 states such as Colorado, Kansas, North Dakota, and Wyoming, while one-way coupling
420 exhibits an overestimation of yields compared to stand-alone (WOFOST) and two-way
421 coupling.

422 For soybeans, the spatial analysis reveals identical yields among stand-alone (WOFOST), one-
423 way, and two-way simulations for both irrigated and rainfed crops. For irrigated crops,
424 simulated yields were overestimated in states like Arkansas and Delaware and underestimated
425 in Kansas and Nebraska compared to reported values. For irrigated and rainfed wheat,
426 simulated yields of the two-way coupling outperform stand-alone WOFOST and one-way
427 coupling, particularly in states like Idaho, Montana, Oregon, and Wyoming. The one-way
428 coupling, lacking feedback from the crop growth model to the hydrological model, leads to an
429 overestimation of rainfed yields across all states compared to stand-alone WOFOST and two-
430 way coupling. This underscores the importance of incorporating two-way interactions and
431 feedback mechanisms for more accurate yield simulation results.

432 **3.2 Evaluation statistics**

433 Table 1 presents model performance metrics (correlation, normalized RMSE and normalized
434 bias), evaluating simulations for the three model setups (i.e. standalone WOFOST, one-way,
435 two-way coupling) for irrigated and rainfed maize, soybean, and wheat.

436 For irrigated crops, simulation approaches exhibit positive correlations. Specifically, for maize,
437 the correlation coefficients are high (0.63), moderate for soybean and rather low for wheat. The
438 normalized root mean square errors (RMSE) remain consistently low, with values ranging from
439 0.13 to 0.18 across three crops, indicating a reasonable fit of the simulated values to the
440 observed data. Moreover, normalized biases are also low, ranging from 0.01 to 0.20. The two-



441 way coupling demonstrates overall slightly lower biases compared to stand-alone and one-way
 442 simulations, particularly for wheat.

443 **Table 1: Model performance metrics (i.e. correlation, normalized RMSE and normalized bias) for**
 444 **simulated irrigated and rainfed maize, soybean, and wheat.**

S.No	Metrics	Maize			Soybean			Wheat		
Irrigated crops		Stand alone	One-way	Two-way	Stand alone	One-way	Two-way	Stand alone	One-way	Two-way
1	Correlation	0.63	0.63	0.63	0.46	0.46	0.45	0.22	0.22	0.24
2	Normalized RMSE	0.13	0.13	0.13	0.06	0.06	0.06	0.18	0.18	0.18
3	Normalized Bias	0.20	0.20	0.20	0.01	0.01	0.01	0.12	0.12	0.06
Rainfed crops		Stand alone	One-way	Two-way	Stand alone	One-way	Two-way	Stand alone	One-way	Two-way
1	Correlation	0.77	0.65	0.77	0.57	0.22	0.33	0.44	0.51	0.55
2	Normalized RMSE	0.22	0.50	0.50	0.42	0.57	0.57	0.37	0.66	0.66
3	Normalized Bias	0.31	1.65	0.84	0.42	0.78	0.63	0.28	0.91	0.32

445
 446 For rainfed crops, the correlation coefficients vary, with two-way coupling displaying the
 447 highest correlations. Higher correlation coefficients are obtained for maize (0.65-0.77)
 448 compared to soybean (0.22-0.57) and wheat (0.44-0.55). Normalized RMSE values are
 449 generally higher in rainfed conditions compared to irrigated, ranging from 0.22 to 0.66.
 450 Normalized biases show variations across simulation approaches and crops, ranging from 0.28
 451 to 1.65. Specifically, one-way coupling exhibits higher biases in rainfed maize, soybean and
 452 wheat compared to stand-alone and two-way simulations.

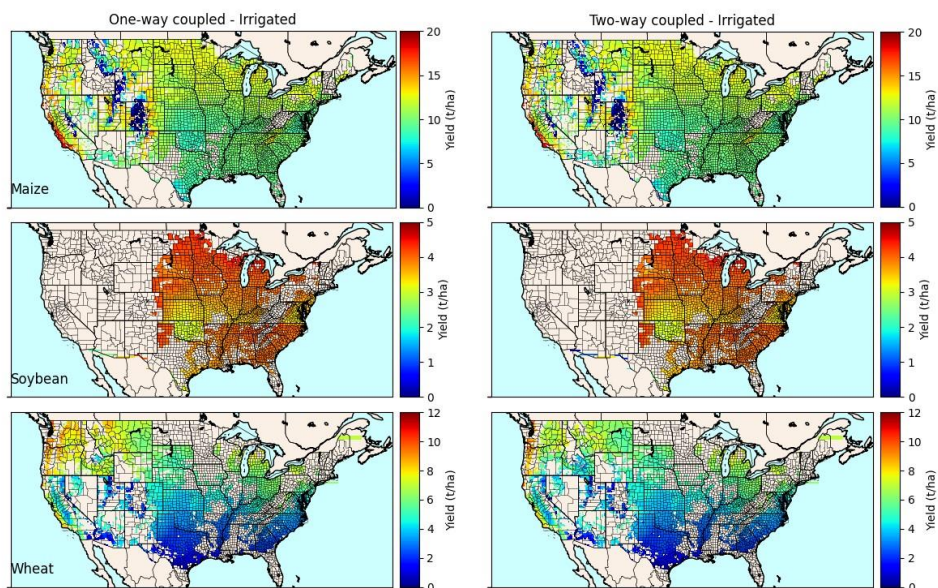
453 Overall, the validation results affirm the overall effectiveness of the simulation approaches in
 454 accurately representing observed irrigated and rainfed crop yields, with stand-alone and two-
 455 way coupling slightly outperforming one-way simulations.

456 **3.3 Relevant feedbacks revealed by two-way coupling between hydrology and crop**
 457 **growth**

458 We further investigated the impact of the developed model coupling by looking at its impact
 459 on simulated crop yield in terms of the CONUS-wide 5-arcminute spatial variation and multi-
 460 year variability. To evaluate the impact of coupling dynamics, we assessed key indicators,
 461 including mean crop yields, the coefficient of variation (CV) of crop yields expressing
 462 interannual variability, and the relative difference in mean and CV between two-way and one-
 463 way couplings.

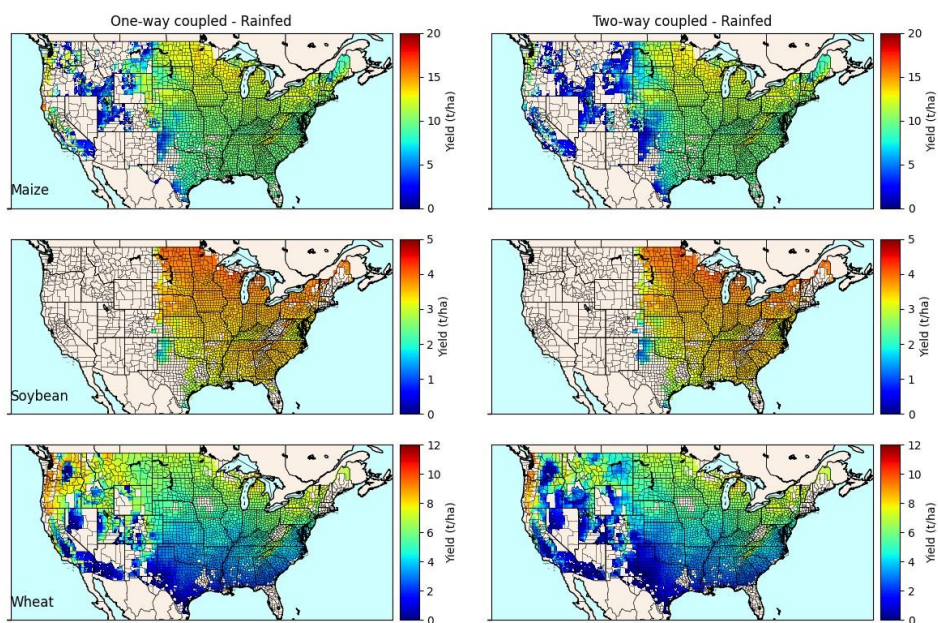


464 Spatial patterns of the 1979-2019 mean simulated crop yields of maize, soybean and wheat are
465 shown under irrigated (Fig. 4) and rainfed (Fig. 5) conditions across the CONUS region. For
466 irrigated crops (Fig. 4), the regions show similar yields for one-way and two-way coupled
467 simulations, which is expected since soil moisture is kept at optimal conditions so that
468 feedbacks from WOFOST to PCR-GLOBWB 2 are inconsequential. For rainfed conditions
469 (Fig. 5), where water availability relies on green water, the yields are comparatively lower than
470 in irrigated conditions. Also, differences between one-way and two-way coupled simulations
471 emerge in the western part of the CONUS. Notably, one-way coupling tends to simulate higher
472 yields for maize and wheat compared to two-way coupling. This discrepancy arises from the
473 transmission of soil moisture from the hydrological to the crop growth model in one-way
474 coupling, without receiving feedback from crop development to the hydrological model. As
475 stated before, this may overestimate soil moisture availability under drier conditions
476 subsequently leading to a likely overestimation of simulated crop yield by the one-way
477 coupling. Clearly, this feedback is more important in the western part of CONUS, which is
478 likely related to larger interannual climate variability (with more dry conditions) compared to
479 the eastern part (see the section hereafter). The larger differences in mean yields for rainfed
480 crops, particularly in the western CONUS, that occur between one-way and two-way coupled
481 simulations are further illustrated by looking at the relative differences between the two
482 coupling methods (see Supplementary Information IV; Fig. S5).



483

484 **Figure 4: Mean irrigated crop yields for maize, soybean, and wheat within CONUS as obtained from one-**
485 **way and two-way coupled simulations for 1979-2019.**



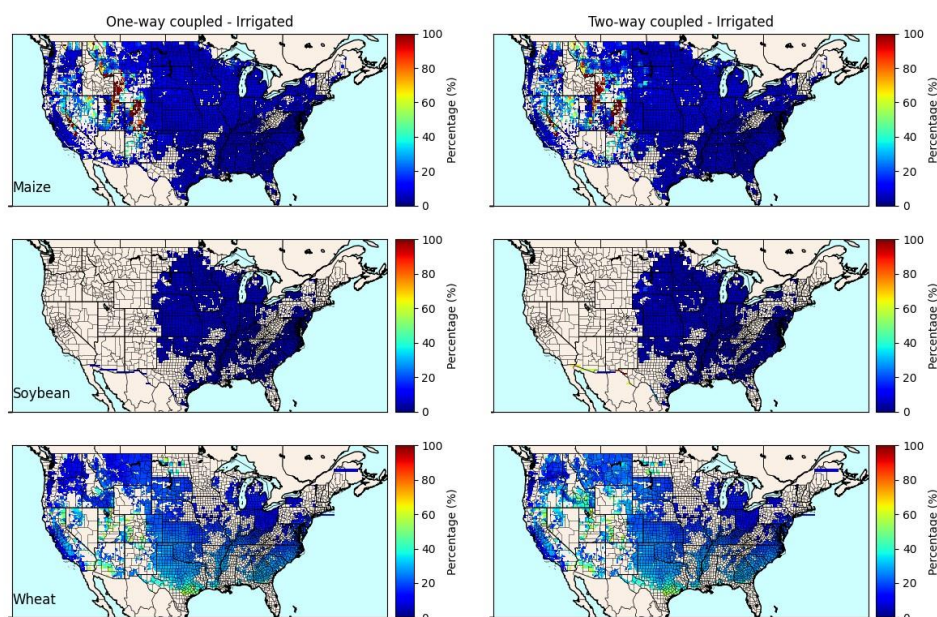
486

487 **Figure 5: Mean rainfed crop yields for maize, soybean, and wheat within CONUS as obtained from one-**
488 **way and two-way coupled simulations for 1979-2019.**



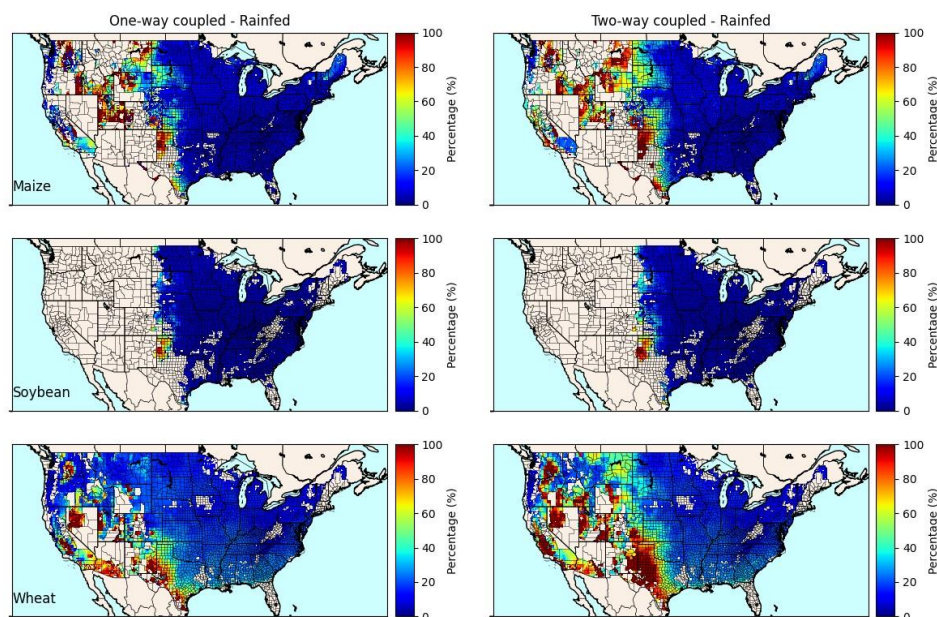
489 Spatial patterns of the coefficient of variation (CV) (in % of the mean) across CONUS for
490 maize, soybean and wheat are shown under irrigated (Fig. 6) and rainfed conditions (Fig. 7)
491 comparing the simulations of the one-way and two-way coupling. High CV values entail a
492 larger inter-annual variability in crop yield.

493 In the eastern part of CONUS, the CV values both in irrigated and rainfed conditions are
494 notably lower, suggesting a more stable and consistent pattern of crop growth in these regions.
495 Conversely, in the mid-western and western CONUS, inter-annual variability is higher, owing
496 to larger inter-annual climate variability in these parts. For irrigated crops, a larger CV is mostly
497 apparent for maize and wheat. For a small number of instances, this could be caused by
498 insufficient irrigation water availability during very dry and hot years, but most likely this is a
499 temperature signal. Also, we note that in these parts of CONUS, some pixels have very low to
500 minimal cropping areas, resulting in more pronounced fluctuations in yields. As can also be
501 seen from Supplementary Information IV Fig. S6, the differences between one-way and two-
502 way coupled runs are generally small, except for some northwestern states.



503

504 **Figure 6: Coefficient of Variation (CV) over 1979-2019 of irrigated crop yields for maize, soybean, and**
505 **wheat within CONUS as obtained under one-way and two-way coupling**



506

507 **Figure 7: Coefficient of Variation (CV) over 1979-2019 of rainfed crop yields for maize, soybean, and wheat**
 508 **within CONUS as obtained under one-way and two-way coupling**

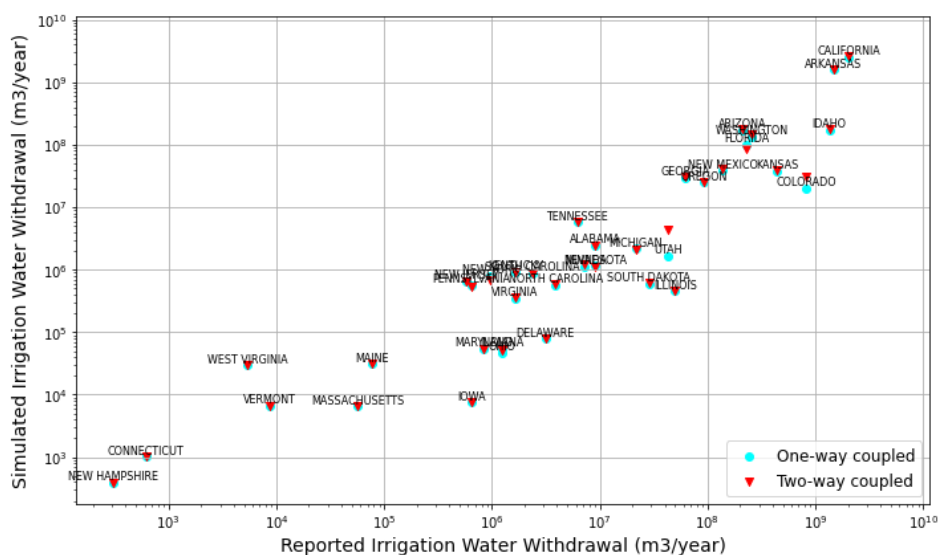
509 Rainfed crops show larger values of CV, especially in the western part of CONUS, reflecting
 510 the larger sensitivity of rainfed agriculture to inter-annual climate variability (Fig. 7). It is also
 511 clear that the simulated inter-annual variability of simulated crop yield is larger for two-way
 512 than for one-way coupling, reflecting the importance of including crop phenology, in particular
 513 variation in rooting depth, when simulating available soil moisture. We also refer to
 514 Supplementary Information IV Fig. S6 for relative differences between the two model coupling
 515 approaches. This larger inter-annual variability also partly explains the lower mean yields for
 516 rainfed crops and two-way coupling as was shown in Fig 5.

517 3.4 Irrigation water use

518 The scatter plot (Fig. 8) shows the relationship between reported USGS (after correction for
 519 area and irrigation efficiency – see 2.4) and simulated irrigation water withdrawals under one-
 520 way and two-way coupling. The plot shows that the simulated irrigation water withdrawals are
 521 correct in order of magnitude when compared to reported data across different states. The
 522 temporal variations (Fig. 9) illustrate that year-to-year changes in total irrigation water
 523 withdrawal over time are small for both one-way and two-way coupling and the reported totals.

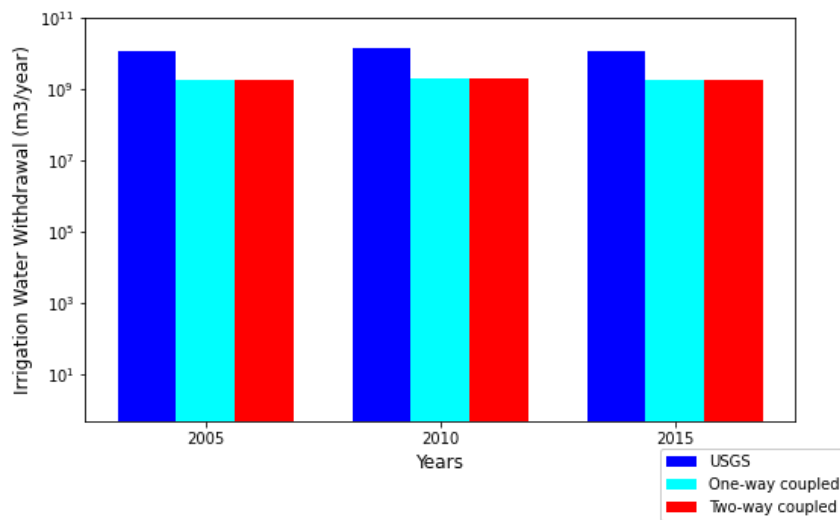


524 Figures 8 and 9 show that irrigation water withdrawal is underestimated in total and for most
525 states. The underestimation of irrigation water use by PCR-GLOBWB 2 was previously noted
526 by Ruess et al., (2023). This underestimation was partly accounted for when using more
527 detailed crop cover data, irrigation efficacies and meteorological forcing than currently used in
528 the global version of PCR-GLOBWB 2.



529

530 **Figure 8: Spatial variation of one-way and two-way irrigation water withdrawal compared with USGS**
531 **water withdrawal data across the CONUS region with a logarithmic scale**



532

533 **Figure 9: Temporal variation of one-way and two-way irrigation water withdrawal compared with USGS**
534 **water withdrawal data of 5-year intervals across the CONUS region with a logarithmic scale**



535 **4 Discussion and Conclusion**

536 In this study, we developed a coupled hydrology-crop model framework to investigate the
537 intricate feedbacks between water availability and crop growth within the CONUS region
538 focusing on maize, soybean and wheat. This discussion delves into the implications of the
539 findings, emphasizing their significance and addressing both methodological considerations
540 and inherent uncertainties.

541 The spatiotemporal analysis of hydrological impacts on crop growth reveals distinctive patterns
542 for both irrigated and rainfed conditions. Notably, the improved performance of the two-way
543 coupling in capturing more realistic yield outcomes for rainfed conditions highlights the
544 importance of incorporating the full feedback loop between hydrology and crop growth. The
545 discrepancy in one-way coupling results, leading to overestimation in simulated compared to
546 reported yields, underscores the importance of feeding back the actual crop phenology to the
547 hydrological model in coupled hydrology-crop growth modelling.

548 Our studies adds to previous work by Droppers et al., (2021), which investigated worldwide
549 water constraints and sustainable irrigation by coupling the Variable Infiltration Capacity
550 (VIC) hydrological model with WOFOST and Zhang et al. (2021) who focused on refining the
551 coupled VIC hydrological model with a crop growth model EPIC by incorporating the
552 evapotranspiration module at a regional scale. In comparison, our research extends the analysis
553 to a finer spatial scale and places a stronger emphasis on the comprehensive integration of
554 feedback loops between hydrology and crop growth. Particularly, we demonstrate the
555 importance of two-way coupling in capturing realistic yield outcomes, which is particularly
556 evident for rainfed crops. This is mainly because the two-way coupled system addresses the
557 influence of crop status on evapotranspiration and rooting depth, thereby impacting soil
558 moisture content, which in turn feed backs on crop growth. The two-way coupling approach
559 provides a more realistic depiction of water availability for crops, which results in larger inter-
560 annual variability and lower mean crop yields when inter-annual climate variability is
561 significant. Including this two-way interaction is particularly important under drier conditions
562 or if the coupled framework is used to assess reduced surface water availability under climate
563 change or the impact of environmental constraints on groundwater and surface water use. The
564 significance of implementing a two-way coupling between hydrology and crop growth is also
565 evident when calculating high-resolution long-term mean crop yields and inter-annual
566 variability of yield, as measured by the coefficient of variation (CV) of simulated yield. In



567 irrigated conditions, both one-way and two-way coupling yield similar results, demonstrating
568 the stability in water availability.

569 Validation results affirm the reliability of the coupled PCR-GLOBWB 2 – WOFOST model
570 framework, demonstrating close agreement with observed data through overall strong positive
571 correlations, low normalized RMSE, and minimal bias. Here, the difference in performance
572 between one-way and two-way coupling is small. In rainfed conditions, where variability is
573 inherent, the better performance of two-way coupling emphasizes the added value of dynamic
574 feedback mechanisms for more accurate simulation results. Even though the stand-alone
575 WOFOST performed similarly to the two-way coupled model framework, the latter is still
576 beneficial for comprehensively understanding the joint impacts on both crop growth and
577 irrigation water use, particularly in situations of limited water availability.

578 While the results of this study offer valuable insights into the coupled hydrology-crop model
579 framework, it is essential to recognize and address the uncertainties associated with the
580 structure and parametrization, as well as inherent limitations in the research. A significant
581 limitation is that the study does not account for potential advancements in agricultural
582 technology and evolving farming practices, which could impact crop yields (section 3.1; Fig.
583 2). The ignorance of technological innovations may contribute to discrepancies between
584 simulated and actual yields.

585 Furthermore, uncertainties linked to input datasets (Porwollik et al., 2017; Roux et al., 2014)
586 such as crop calendars, cultivars and land-use changes introduce potential limitations and
587 implications for the study results. Accurate representations of crop growth dynamics hinge on
588 accurate crop calendar definitions (Wang et al., 2022), encompassing planting, maturation, and
589 harvesting periods. Variations in these timelines due to climate change or evolving agricultural
590 practices potentially introduce uncertainties in yield predictions. Additionally, the assumption
591 of static cultivars neglects potential shifts in agricultural practices or the introduction of new
592 varieties, influencing crop growth responses to environmental stressors over time. Land-use
593 changes further contribute to uncertainties (Prestele et al., 2016; Eckhardt et al., 2003;
594 Dendoncker et al., 2008) as dynamic shifts in agricultural practices alter water demand,
595 evapotranspiration patterns, and overall hydrological dynamics. Ignoring these potential shifts
596 limits the model's ability to capture the complex interactions between water and crop systems,
597 and this should be considered in future development steps.



598 Hence, future work should also consider representing the dynamic nature of crop areas,
599 including both irrigated and rainfed crop harvest areas, as well as the total crop area. The
600 assumption of constant areas, as made in prior studies (Müller et al., 2017; Ai and Hanasaki,
601 2023; Jägermeyr et al., 2021) was based on data availability constraints, but acknowledging
602 the potential variability in these factors over time. Addressing this aspect is crucial for
603 enhancing the accuracy of yield calculations and, consequently, advancing the overall
604 understanding of hydrology-crop growth interactions. The integration of such variability into
605 modelling frameworks is not only essential for improving the accuracy of assessments but also
606 for contributing to an enhanced understanding of the broader water-food nexus.

607 In conclusion, the development and application of the two-way coupled hydrology-crop growth
608 model framework presented in this study represents a significant advancement in our ability to
609 understand the cascading mechanisms and feedbacks between water and crop systems. This
610 versatile framework not only enhances our understanding of the interplay between hydrology
611 and crop growth but, through the sectoral water use modules of PCR-GLOBWB 2, has the
612 necessary components to evaluate large-scale water use management strategies, and simulate
613 the large-scale impacts of informed decision-making under change, particularly when dealing
614 with hydroclimatic extremes.

615 **Author contribution**

616 SC designed the study, performed the analyses, validation and visualization of the results under
617 the supervision of LPHvB, MTHvV and MFPB. SC developed the coupled framework in close
618 collaboration with LPHvB. JA contributed to the conceptualization of software. SC wrote the
619 original draft manuscript and all co-authors reviewed and edited the manuscript.

620 **Code and data availability**

621 The developed coupled PCR-GLOBWB 2-WOFOST model framework is available at
622 <https://zenodo.org/doi/10.5281/zenodo.10681452>. The datasets used in the coupled model
623 framework are available at
624 [https://opendap.4tu.nl/thredds/catalog/data2/pcrglobwb/version_2019_11_beta/pcrglobwb2_i
625 nput/catalog.html](https://opendap.4tu.nl/thredds/catalog/data2/pcrglobwb/version_2019_11_beta/pcrglobwb2_input/catalog.html).

626 **Competing interests**

627 The contact author has declared that none of the authors has any competing interests.

628 **Acknowledgement**



629 The authors acknowledge dr. Bram Droppers (Utrecht University) and dr. Iwan Supit
630 (Wageningen University) for their valuable advices on the WOFOST crop model.

631 **Financial support**

632 This research has been funded by the European Union Horizon Programme GoNexus project
633 (Grant Agreement Number 101003722). MTHvV was financially supported by the Netherlands
634 Scientific Organisation (NWO) by a VIDI grant (VI.Vidi.193.019) and the European Research
635 Council (ERC) under the European Union's Horizon Europe research and innovation program
636 (grant agreement 101039426 B-WEX).

637

638 **5 References**

- 639 Ai, Z., & Hanasaki, N. (2023). Simulation of crop yield using the global hydrological model H08 (crp.v1).
640 *Geoscientific Model Development*, 16(11), 3275–3290. <https://doi.org/10.5194/gmd-16-3275-2023>
- 641 Allen, R. G., Pereira, L. S., Raes, D., & Smith, M. (1998). Crop evapotranspiration-Guidelines for computing crop
642 water requirements-FAO Irrigation and drainage paper 56. Fao, Rome, 300(9), D05109.
- 643 Arata, L., Fabrizi, E., & Skokai, P. (2020). A worldwide analysis of trend in crop yields and yield variability:
644 Evidence from FAO data. *Economic Modelling*, 90, 190–208.
645 <https://doi.org/10.1016/J.ECONMOD.2020.05.006>
- 646 Corona-López, E., Román-Gutiérrez, A. D., Otazo-Sánchez, E. M., Guzmán-Ortiz, F. A., Acevedo-Sandoval, O.
647 A., Corona-López, E. ;, & Román-Gutiérrez, A. D. ; (2021). Water-Food Nexus Assessment in Agriculture:
648 A Systematic Review. *Int. J. Environ. Res. Public Health*, 18, 4983. <https://doi.org/10.3390/ijerph18094983>
- 649 de Wit, A., Boogaard, H., Fumagalli, D., Janssen, S., Knapen, R., van Kraalingen, D., Supit, I., van der Wijngaart,
650 R., & van Diepen, K. (2019). 25 years of the WOFOST cropping systems model. *Agricultural Systems*,
651 168(October 2017), 154–167. <https://doi.org/10.1016/j.agry.2018.06.018>
- 652 Dendoncker, N., Schmit, C., & Rounsevell, M. (2008). Exploring spatial data uncertainties in land-use change
653 scenarios. *International Journal of Geographical Information Science*, 22(9), 1013–1030.
654 <https://doi.org/10.1080/13658810701812836>
- 655 Droppers, B., Supit, I., Van Vliet, M. T. H., & Ludwig, F. (2021). Worldwide water constraints on attainable
656 irrigated production for major crops. *Environmental Research Letters*, 16(5). <https://doi.org/10.1088/1748-9326/abf527>
- 658 Dubois, O. (2011). *The state of the world's land and water resources for food and agriculture: managing systems
659 at risk*. Earthscan.
- 660 Easterling, W. E. (1997). Why regional studies are needed in the development of full-scale integrated assessment
661 modelling of global change processes. *Global Environmental Change*, 7(4), 337–356.
662 [https://doi.org/10.1016/S0959-3780\(97\)00016-2](https://doi.org/10.1016/S0959-3780(97)00016-2)
- 663 Eckhardt, K., Breuer, L., & Frede, H. G. (2003). Parameter uncertainty and the significance of simulated land use
664 change effects. *Journal of Hydrology*, 273(1–4), 164–176. [https://doi.org/10.1016/S0022-1694\(02\)00395-5](https://doi.org/10.1016/S0022-1694(02)00395-5)
665
- 666 Ewert, F., Rötter, R. P., Bindi, M., Webber, H., Trnka, M., Kersebaum, K. C., Olesen, J. E., van Ittersum, M. K.,
667 Janssen, S., Rivington, M., Semenov, M. A., Wallach, D., Porter, J. R., Stewart, D., Verhagen, J., Gaiser,
668 T., Palosuo, T., Tao, F., Nendel, C., ... Asseng, S. (2015). Crop modelling for integrated assessment of risk
669 to food production from climate change. *Environmental Modelling & Software*, 72, 287–303.
670 <https://doi.org/10.1016/J.ENVSOFT.2014.12.003>
- 671 Huang, J., Hartemink, A. E., & Kucharik, C. J. (2021). Soil-dependent responses of US crop yields to climate



- 672 variability and depth to groundwater. *Agricultural Systems*, 190, 103085.
673 <https://doi.org/10.1016/J.AGSY.2021.103085>
- 674 Hutton, E., Piper, M., & Tucker, G. (2020). The Basic Model Interface 2.0: A standard interface for coupling
675 numerical models in the geosciences. *Journal of Open Source Software*, 5(51), 2317.
676 <https://doi.org/10.21105/joss.02317>
- 677 IRENA. (2015). Renewable energy in the water, energy and food nexus. *International Renewable Energy Agency*,
678 *January*, 1–125.
- 679 Jackson, N. D., Konar, M., Debaere, P., & Sheffield, J. (2021). Crop-specific exposure to extreme temperature
680 and moisture for the globe for the last half century. *Environmental Research Letters*, 16(6), 064006.
681 <https://doi.org/10.1088/1748-9326/ABF8E0>
- 682 Jägermeyr, J., Pastor, A., Biemans, H., & Gerten, D. (2017). Reconciling irrigated food production with
683 environmental flows for Sustainable Development Goals implementation. *Nature Communications*,
684 8(May), 1–9. <https://doi.org/10.1038/ncomms15900>
- 685 Jägermeyr, J., Müller, C., Ruane, A. C., Elliott, J., Balkovic, J., Castillo, O., ... & Rosenzweig, C. (2021). Climate
686 impacts on global agriculture emerge earlier in new generation of climate and crop models. *Nature*
687 *Food*, 2(11), 873–885.
- 688 Lange, S., Menz, C., Gleixner, S., Cucchi, M., Weedon, G. P., Amici, A., Bellouin, N., Schmied, H. M., Hersbach,
689 H., Buontempo, C., & Cagnazzo, C. (2021). (2021). *Lange, S., Menz, C., Gleixner, S., Cucchi, M., Weedon,*
690 *G. P., Amici, A., Bellouin, N., Schmied, H. M., Hersbach, H., Buontempo, C., & Cagnazzo, C. (2021).*
691 *WFDE5 over land merged with ERA5 over the ocean (W5E5 v2.0)*. 2021.
- 692 Leclère, D., Havlík, P., Fuss, S., Schmid, E., Mosnier, A., Walsh, B., Valin, H., Herrero, M., Khabarov, N., &
693 Obersteiner, M. (2014). Climate change induced transformations of agricultural systems: Insights from a
694 global model. *Environmental Research Letters*, 9(12). <https://doi.org/10.1088/1748-9326/9/12/124018>
- 695 McMillan, H. K., Westerberg, I. K., & Krueger, T. (2018). Hydrological data uncertainty and its implications.
696 *Wiley Interdisciplinary Reviews: Water*, 5(6), 1–14. <https://doi.org/10.1002/WAT2.1319>
- 697 Momblanch, A., Papadimitriou, L., Jain, S. K., Kulkarni, A., Ojha, C. S. P., Adedoye, A. J., & Holman, I. P.
698 (2019). Science of the Total Environment Untangling the water-food-energy-environment nexus for global
699 change adaptation in a complex Himalayan water resource system. *Science of the Total Environment*, 655,
700 35–47. <https://doi.org/10.1016/j.scitotenv.2018.11.045>
- 701 Mortada, S., Abou Najm, M., Yassine, A., El Fadel, M., & Alamiddine, I. (2018). Towards sustainable water-
702 food nexus: An optimization approach. *Journal of Cleaner Production*, 178, 408–418.
703 <https://doi.org/10.1016/J.JCLEPRO.2018.01.020>
- 704 Müller, C., Elliott, J., Chryssanthacopoulos, J., Arneth, A., Balkovic, J., Ciais, P., Deryng, D., Folberth, C.,
705 Glotter, M., Hoek, S., Iizumi, T., Izaurralde, R. C., Jones, C., Khabarov, N., Lawrence, P., Liu, W., Olin,
706 S., Pugh, T. A. M., Ray, D. K., ... Yang, H. (2017). Global gridded crop model evaluation: Benchmarking,
707 skills, deficiencies and implications. *Geoscientific Model Development*, 10(4), 1403–1422.
708 <https://doi.org/10.5194/gmd-10-1403-2017>
- 709 Peckham, S. D., Hutton, E. W. H., & Norris, B. (2013). A component-based approach to integrated modeling in
710 the geosciences: The design of CSDMS. *Computers & Geosciences*, 53, 3–12.
711 <https://doi.org/10.1016/J.CAGEO.2012.04.002>
- 712 Portmann, F. T., Siebert, S., & Döll, P. (2010). MIRCA2000—Global monthly irrigated and rainfed crop areas
713 around the year 2000: A new high-resolution data set for agricultural and hydrological modeling. *Global*
714 *Biogeochemical Cycles*, 24(1), 1–24. <https://doi.org/10.1029/2008gb003435>
- 715 Porwollik, V., Müller, C., Elliott, J., Chryssanthacopoulos, J., Iizumi, T., Ray, D. K., Ruane, A. C., Arneth, A.,
716 Balkovič, J., Ciais, P., Deryng, D., Folberth, C., Izaurralde, R. C., Jones, C. D., Khabarov, N., Lawrence, P. J.,
717 Liu, W., Olin, A. M., Reddy, A., ... Wu, X. (2017). Spatial and temporal uncertainty of crop yield
718 aggregations. *European Journal of Agronomy*, 88, 10–21. <https://doi.org/10.1016/J.EJA.2016.08.006>
- 719 Prestele, R., Alexander, P., Rounsevell, M. D. A., Arneth, A., Calvin, K., Doelman, J., Eitelberg, D. A., Engström,
720 K., Fujimori, S., Hasegawa, T., Havlik, P., Humpenöder, F., Jain, A. K., Krisztin, T., Kyle, P., Meiyappan,
721 P., Popp, A., Sands, R. D., Schaldach, R., ... Verburg, P. H. (2016). Hotspots of uncertainty in land-use and



- 722 land-cover change projections: a global-scale model comparison. *Global Change Biology*, 22(12), 3967–
723 3983. <https://doi.org/10.1111/gcb.13337>
- 724 Roux, S., Brun, F., & Wallach, D. (2014). Combining input uncertainty and residual error in crop model
725 predictions: A case study on vineyards. *European Journal of Agronomy*, 52, 191–197.
726 <https://doi.org/10.1016/J.EJA.2013.09.008>
- 727 Ruess, P. J., Konar, M., Wanders, N., & Bierkens, M. (2023). Irrigation by Crop in the Continental United States
728 From 2008 to 2020. *Water Resources Research*, 59(2), 1–19. <https://doi.org/10.1029/2022WR032804>
- 729 Shafiei, M., Ghahraman, B., Saghafian, B., Davary, K., Pande, S., & Vazifedoust, M. (2014). Uncertainty
730 assessment of the agro-hydrological SWAP model application at field scale: A case study in a dry region.
731 *Agricultural Water Management*, 146, 324–334. <https://doi.org/10.1016/J.AGWAT.2014.09.008>
- 732 Siad, S. M., Iacobellis, V., Zdruli, P., Gioia, A., Stavi, I., & Hoogenboom, G. (2019). A review of coupled
733 hydrologic and crop growth models. *Agricultural Water Management*, 224, 105746.
734 <https://doi.org/10.1016/J.AGWAT.2019.105746>
- 735 Sophocleous, M. (2004). *Global and Regional Water Availability and Demand : Prospects for the Future*. 13(2).
- 736 Supit, I., Hooijer, A. A., & van Diepen, C. A. (Eds. . (1994). System description of the WOFOST 6.0 crop
737 simulation model implemented in CGMS Vol. 1: *Theory and Algorithms*. *EUR Publication 15956*,
738 *Agricultural Series, Luxembourg*, 146 Pp., 1(October 2015), 181.
739 <https://cir.nii.ac.jp/crid/1573950399770954368>
- 740 Sutanudjaja, E. H., Van Beek, R., Wanders, N., Wada, Y., Bosmans, J. H. C., Drost, N., Van Der Ent, R. J., De
741 Graaf, I. E. M., Hoch, J. M., De Jong, K., Karssenberg, D., López López, P., Peßenteiner, S., Schmitz, O.,
742 Straatsma, M. W., Vannamete, E., Wisser, D., & Bierkens, M. F. P. (2018). PCR-GLOBWB 2: A 5 arcmin
743 global hydrological and water resources model. *Geoscientific Model Development*, 11(6), 2429–2453.
744 <https://doi.org/10.5194/gmd-11-2429-2018>
- 745 Tompkins, E. L., & Adger, W. N. (2004). *Does Adaptive Management of Natural Resources Enhance Resilience*
746 *to Climate Change ?* 9(2).
- 747 Tsarouchi, G. M., Buytaert, W., & Mijic, A. (2014). *Coupling a land-surface model with a crop growth model to*
748 *improve ET flux estimations in the Upper Ganges basin , India*. 4223–4238. [https://doi.org/10.5194/hess-](https://doi.org/10.5194/hess-18-4223-2014)
749 [18-4223-2014](https://doi.org/10.5194/hess-18-4223-2014)
- 750 USGS, 2023. Water use in the United States, from USGS Water-Science School. 1–2.
751 <https://water.usgs.gov/watuse/data/index.html>
- 752 USDA: <https://quickstats.nass.usda.gov/>, last access: 06 February 2024.
- 753 Veetil, A. V., Mishra, A. K., & Green, T. R. (2022). Explaining water security indicators using hydrologic and
754 agricultural systems models. *Journal of Hydrology*, 607, 127463.
755 <https://doi.org/10.1016/J.JHYDROL.2022.127463>
- 756 Vörösmarty, C. J., Green, P., Salisbury, J., & Lammers, R. B. (2000). Global water resources: Vulnerability from
757 climate change and population growth. *Science*, 289(5477), 284–288.
758 <https://doi.org/10.1126/science.289.5477.284>
- 759 Wang, X., Folberth, C., Skalsky, R., Wang, S., Chen, B., Liu, Y., Chen, J., & Balkovic, J. (2022). Crop calendar
760 optimization for climate change adaptation in rice-based multiple cropping systems of India and
761 Bangladesh. *Agricultural and Forest Meteorology*, 315, 108830.
762 <https://doi.org/10.1016/J.AGRFORMET.2022.108830>
- 763 WOFOST Crop Parameters: https://github.com/ajwdewit/WOFOST_crop_parameters, last access: 06 February
764 2024.
- 765 Zhang, Y., Wu, Z., Singh, V. P., He, H., He, J., Yin, H., & Zhang, Y. (2021). Coupled hydrology-crop growth
766 model incorporating an improved evapotranspiration module. *Agricultural Water Management*, 246(1),
767 106691. <https://doi.org/10.1016/j.agwat.2020.106691>
- 768